

Colloidal inverse bicontinuous cubic membranes of block copolymers with tunable surface functional groups

Yunju La¹, Chiyoung Park¹, Tae Joo Shin³, Sang Hoon Joo^{1,2}, Sebyung Kang² and Kyoung Taek Kim^{1,2,4*}

Analogous to the complex membranes found in cellular organelles, such as the endoplasmic reticulum, the inverse cubic mesophases of lipids and their colloidal forms (cubosomes) possess internal networks of water channels arranged in crystalline order, which provide a unique nanospace for membrane-protein crystallization and guest encapsulation. Polymeric analogues of cubosomes formed by the direct self-assembly of block copolymers in solution could provide new polymeric mesoporous materials with a three-dimensionally organized internal maze of large water channels. Here we report the self-assembly of amphiphilic dendritic-linear block copolymers into polymer cubosomes in aqueous solution. The presence of precisely defined bulky dendritic blocks drives the block copolymers to form spontaneously highly curved bilayers in aqueous solution. This results in the formation of colloidal inverse bicontinuous cubic mesophases. The internal networks of water channels provide a high surface area with tunable surface functional groups that can serve as anchoring points for large guests such as proteins and enzymes.

Synthesized by covalently connecting both the hydrophilic and hydrophobic blocks, amphiphilic block copolymers self-assemble in solution to form polymer micelles and vesicles in an analogous fashion to lipids. Previously, precise control of the size, shape and function of these polymer nanostructures has been demonstrated by adjusting the molecular architecture of the block copolymers. The design rules for this were drawn using an analogy to the relationship between the molecular architecture and the morphology of lipidic assemblies^{1–7}. In addition to the morphological diversity, recent efforts have been placed on polymer micelles and vesicles with well-defined internal order within the hydrophobic compartment. Such an ordered array of chemical components is expected to offer benefits for potential applications for example biochemical reactors, delivery vehicles and nanotemplates^{8–12}. In an analogous fashion to the templated synthesis of inorganic mesoporous materials, these compositional arrays could be translated into physical structures, such as a mesoporous network, by selectively removing the labile polymer domains^{13,14}. The direct formation of mesoporous polymers is highly desirable¹⁵, but has remained a challenge, especially for the solution self-assembly of block copolymers.

A binary mixture of water and lipid, such as glycerol monooleate, exhibits the formation of various inverse bicontinuous crystalline phases, in which the infinite network of water channels is arranged into crystalline lattices^{16,17}. These lipid cubic membranes are found in cellular organelles such as the endoplasmic reticulum¹⁸. Colloidal forms of cubic lipid membranes also appear transiently during fat-digestion processes that convert oil into lipids¹⁹. These complex lipid bilayers have attracted recent attention, in particular for their structural characteristics^{18,20}. The inverse cubic mesophases of lipids and their colloidal forms (cubosomes)^{21,22} provide a unique nanospace for membrane-protein crystallization and guest encapsulation^{23–26}. In solution, block copolymers behave in an analogous fashion to lipids with a greater length scale, which results in micellar and vesicular structures with the desired chemical and physical

properties. In this respect, the self-assembly of block copolymers to give cubosome structures is an attractive goal. Polymeric counterparts of these structures could lead to the direct access of highly defined mesoporous polymer materials with the desired physical and chemical properties owing to the diverse chemical structures of block-copolymer building blocks.

Block copolymers may form inverse cubic mesophases in concentrated solution^{27–29}. Analogues of cubosomes have been observed previously from the self-assembly of synthetic macromolecules such as triblock copolymers, semi-crystalline brush block copolymers and dendritic amphiphiles^{8,30–35}. In spite of these reports, a clear rationale that underlies the self-assembly of block copolymers to give inverse mesophases in solution has not been proposed³⁶. Consequently, the design of block copolymers to form preferentially complex bilayers and inverted mesophases in solution remains unexplored. We describe here the direct self-assembly of dendritic-linear block copolymers in aqueous solution into colloidal particles of bicontinuous cubic membranes (polymer cubosomes) with the desired crystalline lattice. Three inverse bicontinuous cubic phases (primitive cubic, double diamond and gyroid) were identified from the polymer cubosomes of our dendritic-linear block copolymers depending on the architecture of the dendritic scaffold in the hydrophilic block. Our experimental results strongly suggest that the presence of an accurately defined dendritic architecture in the hydrophilic block is a key structural element of the solution self-assembly of amphiphilic block copolymers into inverse bicontinuous mesophases. We also show that the bilayer membranes consisting of polymer cubosomes can be equipped with desired surface functional groups, which makes polymer cubosomes an interesting porous platform to host macromolecular guests such as proteins and enzymes.

Result and discussion

Self-assembly of dendritic-linear block copolymers into polymer cubosomes. In this study, we synthesized isomers of

¹Department of Chemistry, Ulsan National Institute of Science and Technology, 50 UNIST Road, Ulsan 689-798, Korea, ²School of Nano-Bioscience and Chemical Engineering, Ulsan National Institute of Science and Technology, 50 UNIST Road, Ulsan 689-798, Korea, ³Pohang Accelerator Laboratory, POSTECH, Pohang 790-784, Korea, ⁴KIST-UNIST-Ulsan Center for Convergence Materials, Ulsan 689-798, Korea. *e-mail: ktkim@unist.ac.kr

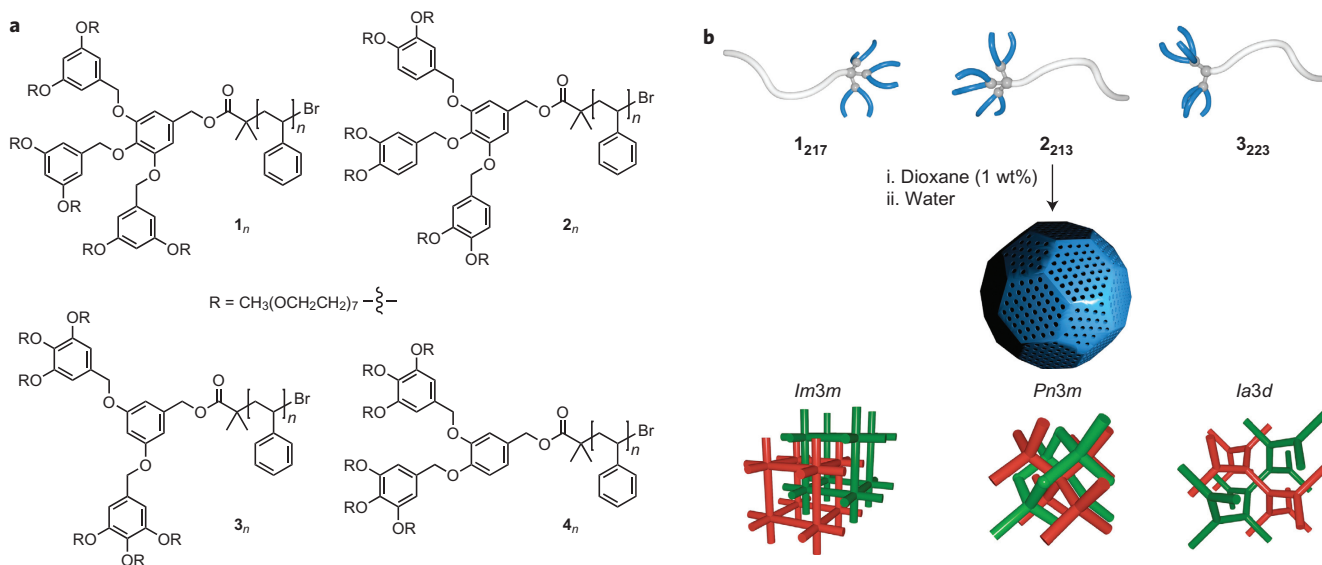


Figure 1 | Chemical structures and schematic diagrams of dendritic-linear block copolymers and their self-assembly. **a**, Chemical structures of block copolymers 1_n and 2_n constructed from the two isomers of benzyl ether dendrons that possess peripheral PEG chains at the 3,5-positions (1_n) and 3,4-positions (2_n) of the outer phenyl groups, and 3_n and 4_n built from dendritic blocks that consist of two peripheral 3,4,5-PEG-benzyl ether units at the 3,5 (3_n) and 3,4 (4_n) positions of the central benzyl unit. The subscript n denotes the DP of the PS block. **b**, A schematic representation of the self-assembly of dendritic-linear block copolymers into polymer cubosomes in dilute aqueous solution. The lattice diagrams at the bottom show bicontinuous cubic internal structures of the polymer cubosomes ($Im3m$, $Pn3m$ and $Ia3d$) investigated in this study. For clarity, the bilayers that surround the water channels are omitted. The green- and red-coloured regions indicate two non-intersecting networks of water channels within the bicontinuous structures.

second-generation benzyl ether dendrons with six water-soluble peripheral poly(ethylene glycol) (PEG) chains (Fig. 1 and Supplementary Figs 1 and 2). Each peripheral PEG chain had the same number-average molecular weight (M_n) of 350 g mol⁻¹ (number of repeat units or degree of polymerization (DP_n) was seven). These dendritic isomers were converted into macroinitiators for the atom-transfer radical polymerization of styrene³⁷. The hydrophobic polystyrene (PS) block was grown from the focal point of the hydrophilic dendrons with a controlled molecular weight and narrow size distribution. The DP_n of the PS blocks was controlled to fit a range of about 180–240, so that the block ratio of the resulting dendritic-linear block copolymers, defined as the ratio of the molecular weight of the PEG domain to that of the PS block (f_{PEG}), was in the range of about 8–11% to ensure that the block copolymers predominantly self-assemble into bilayer structures³⁸.

All block copolymers were self-assembled by a simple cosolvent method⁵: to a 1,4-dioxane solution of a block copolymer (typically 1 wt%) was added an equal volume of water for a period of two hours, followed by a dialysis against water. We first studied aqueous suspension solutions prepared from a series of dendritic-linear block copolymers 1_n (Fig. 1, where the subscript n denotes the DP_n of the PS block). On transmission electron microscopy (TEM), the suspension solution of 1_{185} ($M_n = 19,100$ g mol⁻¹, polydispersity index (D) = 1.09, $f_{\text{PEG}} = 10.9\%$) showed bilayer structures, flat and folded lamella, along with polymer vesicles (Supplementary Fig. 7). However, on an increase in the length of the PS block, the block copolymer 1_{217} ($M_n = 21,300$ g mol⁻¹, $D = 1.07$, $f_{\text{PEG}} = 9.3\%$) formed large colloidal particles with an average diameter of 6.2 μm (polydispersity (PD) = 0.27), as determined by dynamic light scattering (DLS) measurements.

The detailed morphology of the colloidal particles was studied using TEM and scanning electron microscopy (SEM). The TEM images of the dried suspension of 1_{217} showed colloidal particles (Fig. 2a) that had bicontinuous internal structures resembling those seen in cryogenic TEM images of lipid cubosomes³⁹. Therefore, owing to this structural similarity we named our colloidal

particles as polymer cubosomes^{8,32}. The SEM images of the polymer cubosomes of 1_{217} (coated with a 3 nm thick layer of Pt) clearly revealed details of their hierarchical structure. Low-resolution SEM images showed spherical polymer cubosomes with an average diameter corresponding to that obtained with DLS (Fig. 2c). To our surprise, high-resolution SEM (HR-SEM) images revealed that the polymer cubosomes had bicontinuous internal structures enclosed in a perforated lamellar shell, the surface of which was inundated with evenly distributed pores approximately 10 nm in diameter (Fig. 2e). From the SEM and TEM images, the thickness of the perforated shell was estimated to be ~15 nm, which suggests that it was a bilayer of 1_{217} (Supplementary Fig. 10). SEM images of the polymer cubosomes that fractured during the sample preparation showed a highly ordered crystalline structure residing in the perforated bilayer shell (Fig. 3a and Supplementary Fig. 10), which was consistent with the TEM observations.

The internal order of the polymer cubosomes of 1_{217} was studied using synchrotron small-angle X-ray scattering (SAXS, PLS-II 9A beamline). The SAXS results of the dried polymer cubosomes of 1_{217} showed a set of peaks that corresponded to the primitive cubic ($Im3m$) symmetry (lattice parameter (a) = 93.4 nm (Fig. 3c)), which was in agreement with the TEM and SEM images and confirmed the presence of a highly regular and long-range cubic arrangement of water channels. The structural hierarchy of the polymer cubosomes of 1_{217} , with a bicontinuous cubic internal structure enclosed within a perforated bilayer shell, suggested that the polymer cubosomes should be mesoporous on withdrawal from water. Under ambient conditions, it was found that the dried polymer cubosomes were physically robust because of the high glass-transition temperature (T_g) of the hydrophobic PS block of high molecular weight ($T_g = 101^\circ\text{C}$). The mesoporous nature of the dried polymer cubosomes of 1_{217} were substantiated by N₂-adsorption experiments at 77 K. Type IV adsorption isotherms with type H2 hysteresis loops were observed, with a Brunauer-Emmett-Teller (BET) surface area of 112 m² g⁻¹ and a pore volume of 1.01 cm³ g⁻¹ (Fig. 3e). The Barrett-Joyner-Halenda (BJH)

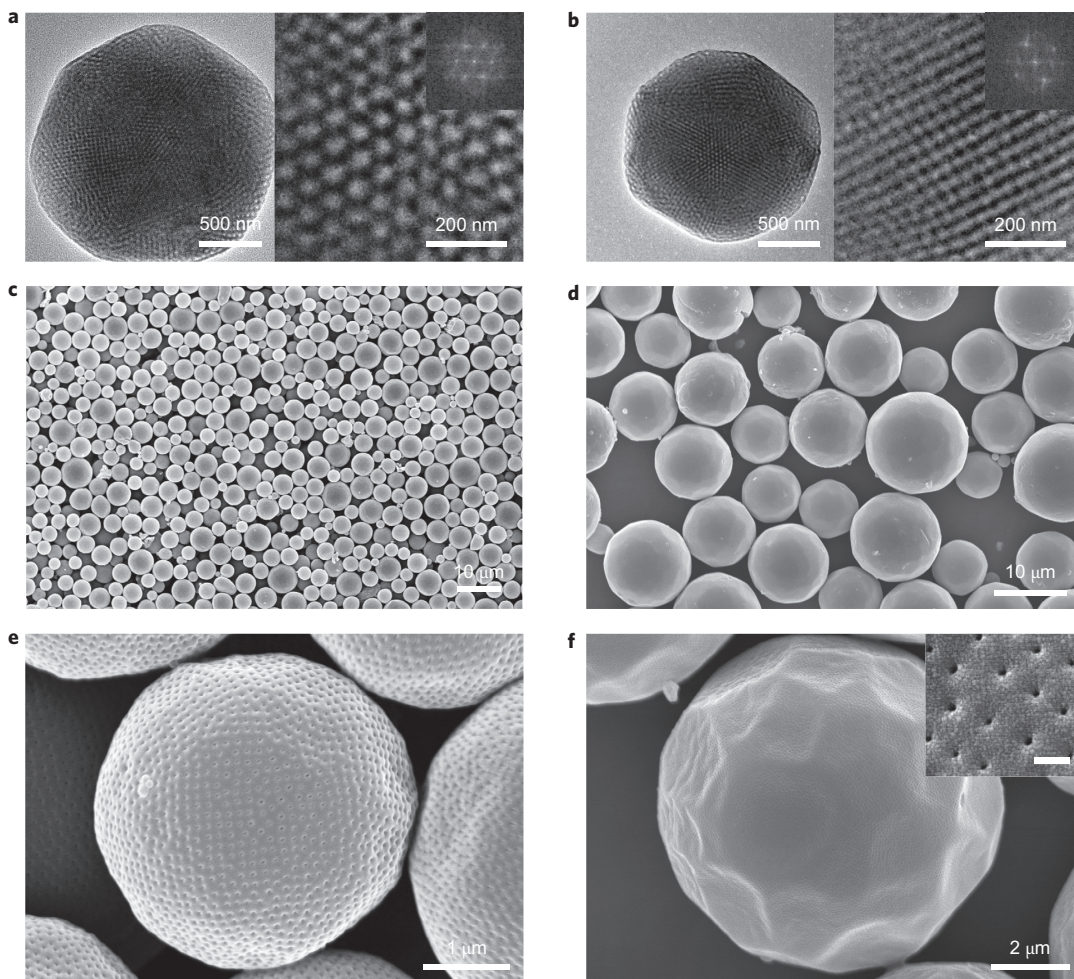


Figure 2 | Representative SEM and TEM images of the polymer cubosomes. **a**, TEM images showing the internal structure of the polymer cubosomes of **1₂₁₇** (left). The magnified view of the internal structures and the fast Fourier transform (FFT) (inset) show a cubic (*Im3m*) lattice viewed in the [111] direction (right). **b**, TEM images of polymer cubosomes of **2₂₁₃**. The right image shows the view of a double diamond (*Pn3m*) lattice viewed in the [001] direction and the FFT of the image. **c,d**, Low-magnification SEM images of polymer cubosomes of **1₂₁₇** (**c**) and **2₂₁₃** (**d**). **e**, SEM image of the polymer cubosome of **1₂₁₇** showing a spherical morphology and the perforated shell enclosing the internal bicontinuous structure. **f**, SEM images of the polymer cubosomes of **2₂₁₃**. The inset shows a magnified view of the surface pores (scale bar, 100 nm).

pore-size distribution curve showed a broad range of pores with a peak diameter of 50 nm (Supplementary Fig. 11).

The effect of the architecture of block copolymers on self-assembly. Based on these findings, we surmised that a change in the architecture of the dendritic block, with the length of the PS block kept constant, might enable controlled alteration of the molecular packing of the block copolymers in the condensed phase. As the molecular weights of both dendritic and PS blocks are fixed to constant values, this change would differentiate the local curvature without radically altering the overall morphology of self-assembled bilayers³⁷, which could induce phase transitions between different bicontinuous cubic phases. This assumption might be justified by Langmuir isotherm experiments carried out on two structural isomers, **1₂₁₇** and **2₂₁₃** ($M_n = 21,300 \text{ g mol}^{-1}$, $D = 1.08$, $f_{\text{PEG}} = 9.4\%$ (Fig. 1)), which gave the area per molecule in a monolayer at an air–water interface of $1,370 \text{ \AA}^2$ for **1₂₁₇** and $1,530 \text{ \AA}^2$ for **2₂₁₃** (Supplementary Fig. 12). The linear diblock copolymer with similar molecular weights on both blocks (PEG₄₅-PS₂₁₀) showed a molecular area of 950 \AA^2 .

TEM images of the aqueous suspension of **2₂₁₃**, prepared under the same conditions as for **1₂₁₇**, showed polymer cubosomes (average diameter $7.9 \mu\text{m}$, PD = 0.22, determined by DLS) with

structural characteristics similar to those of **1₂₁₇** (Fig. 2b). SEM images of the polymer cubosomes of **2₂₁₃** showed the presence of an internal structure of the double diamond lattice (*Pn3m*) (Fig. 3b), which was later confirmed by the SAXS results obtained from the dried polymer cubosomes of **2₂₁₃** ($a = 49.5 \text{ nm}$ (Fig. 3d)). The dried polymer cubosomes of **2₂₁₃** were also found to be mesoporous by N₂-adsorption experiments at 77 K (BET surface area of $101 \text{ m}^2 \text{ g}^{-1}$ and pore volume of $0.99 \text{ cm}^3 \text{ g}^{-1}$, a peak pore diameter of 37 nm from the BJH curve (Fig. 3e and Supplementary Fig. 11)).

Encouraged by this result, we decided to investigate further the possibility of finding other inverse mesophases by synthesizing another set of block copolymers, **3_n** and **4_n**, built from the hydrophilic dendritic blocks with two peripheral 3,4,5-PEG-benzyl ether units at the 3,5- (**3_n**) and 3,4- (**4_n**) positions of the central benzyl unit, respectively (DP_n of PEG = 7 (Fig. 1)). Under the same conditions, both block copolymers self-assembled into polymer cubosomes. SAXS and SEM studies of the polymer cubosomes of **3₂₂₃** ($M_n = 23,700 \text{ g mol}^{-1}$, $D = 1.06$, $f_{\text{PEG}} = 9.1\%$) confirmed the internal lattice of gyroid structures (*Ia3d*, $a = 82.3 \text{ nm}$ (Fig. 4c)), and the polymer cubosomes of **4₂₂₂** ($M_n = 23,400 \text{ g mol}^{-1}$, $D = 1.06$, $f_{\text{PEG}} = 9.1\%$) showed the internal bicontinuous structures of *Pn3m* symmetry ($a = 52.3 \text{ nm}$ (Supplementary Fig. 13)). These polymer cubosomes were also found to be mesoporous by

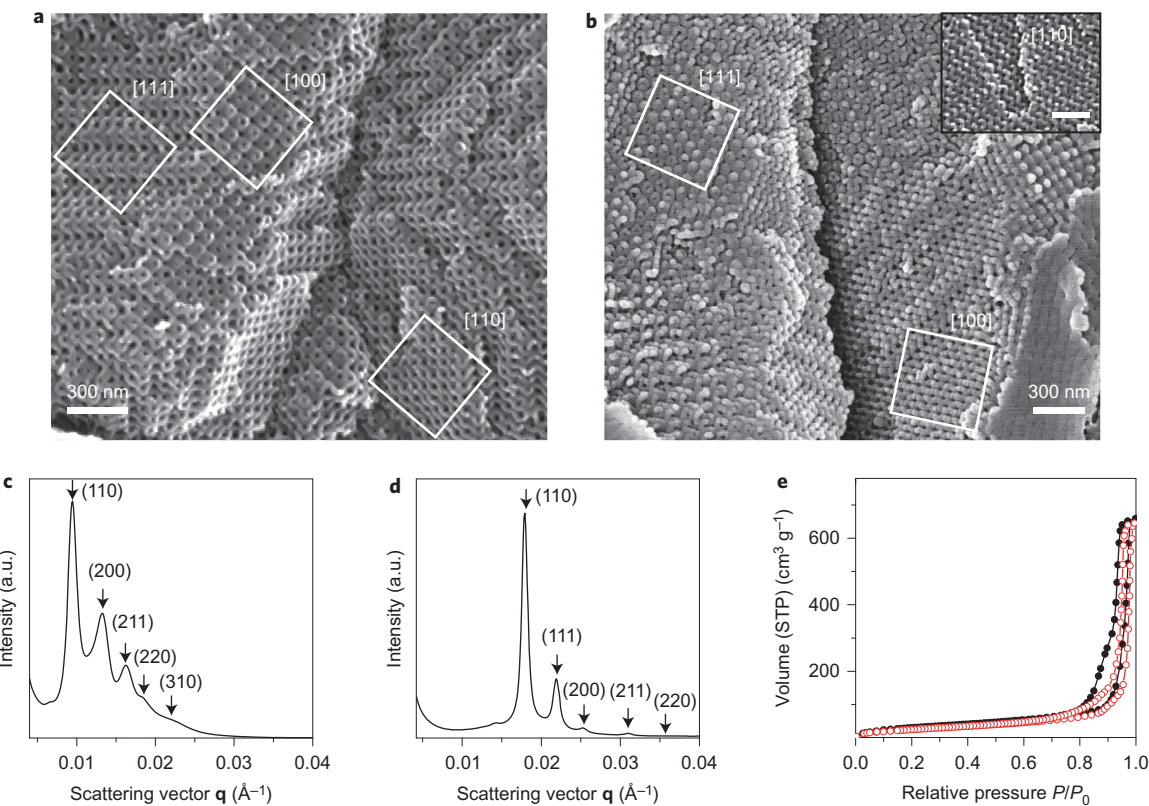


Figure 3 | Structural analysis of the polymer cubosomes. **a**, HR-SEM image of the bicontinuous cubic internal structure of the polymer cubosome of **1₂₁₇** having a primitive cubic ($Im\bar{3}m$) lattice. The internal structures were observed from the fractured polymer cubosomes during the sample preparation. The views in the [100], [110] and [111] directions are highlighted by white squares. **b**, HR-SEM images of a double diamond ($Pn\bar{3}m$) internal structure of the polymer cubosomes of **2₂₁₃**. Views in the [111] and [100] directions are highlighted by white squares. The inset shows a view in the [110] direction (scale bar, 200 nm). **c**, The SAXS result of the dried polymer cubosomes of **1₂₁₇**, which indicates the primitive cubic ($Im\bar{3}m$) lattice (lattice parameter, $a = 93.4$ nm). **d**, The SAXS result of the dried polymer cubosomes of **2₂₁₃** shows the double diamond ($Pn\bar{3}m$) lattice ($a = 49.5$ nm). **e**, N_2 adsorption-desorption isotherms of the dried polymer cubosomes of **1₂₁₇** (filled circles) and **2₂₁₃** (open circles) measured at 77 K. a.u., arbitrary units; STP, standard temperature and pressure.

N_2 -adsorption/desorption experiments, which showed similar results to those obtained previously (Fig. 4).

Given that linear diblock copolymers $PEG_{45}-PS_n$ possessing similar f_{PEG} values to those of dendritic-linear block copolymers ($n = \sim 180-270$, $f_{PEG} = \sim 7.1-10.6\%$), only formed polymer vesicles under same experimental conditions³⁸ (Supplementary Fig. 8), our results suggested that the presence of the dendritic benzyl ether architecture in the hydrophilic block plays an essential role in the formation of inverse bicontinuous phases in dilute solution.

The structure-morphology relationship of lipidic self-assembly could be qualitatively explained by the molecular architecture of the lipid, defined by the critical packing factor ($P = v/a_0 l$, where v is the volume of the hydrophobic chain, a_0 is the effective area of a hydrophilic headgroup and l is the effective length of the molecule)¹. As P increases, the morphology of the self-assembled structure of lipids transforms from spheres to rod-like micelles and vesicles. When P exceeds 1, the self-assembled bilayer of lipids develops a negative curvature, which results in the formation of inverse bicontinuous structures^{17,40}. Our experimental results showed a close resemblance to the self-assembly of lipids such as glyceryl monooleate, which exhibited the formation of inverse bicontinuous cubic structures described as minimal surface structures of negative Gaussian curvature and include double-diamond ($Pn\bar{3}m$), gyroid ($Ia\bar{3}d$) and primitive cubic ($Im\bar{3}m$) phases^{16,17}.

Mechanism of the formation of polymer cubosomes. To investigate the details of the self-assembly of dendritic-linear

block copolymers in dilute solution, we used a kinetic quenching method by taking drops (~ 20 μ l) of suspension solution during the different stages of water addition, followed by immediate dilution with excess water (2 ml). This method enabled the capture of a snapshot of the self-assembly that resulted from vitrification of the high molecular weight PS blocks at the time of dilution with excess water. Even in the early stage of self-assembly (water content $\sim 15\%$), we observed similar polymer cubosomes with less well-defined internal structures compared to those observed at a 50% water content (Supplementary Fig. 14) by TEM experiments. DLS results did not show any gradual increase of the average diameter during water addition. The reduction of the rate of water addition (20% of the typical rate) into a dioxane solution of block copolymers did not alter the internal phase, but only affected the average diameter and size distribution of polymer cubosomes. These results ruled out the possibility that the polymer cubosomes were formed during dialysis, and also suggested that the formation of polymer cubosomes was a result of the direct self-assembly of dendritic-linear block copolymers into mesophases rather than that of the secondary self-assembly of bilayers or polymersomes into bicontinuous structures.

The phase behaviour of dendritic-linear block copolymers in aqueous solution was affected mainly by their block ratio. For example, both **1₂₃₂** and **2₂₄₅** (f_{PEG} of 8.9% for **1₂₃₂** and 8.4% for **2₂₄₅**) showed the emergence of an inverted hexagonal phase within the polymer cubosomes (Supplementary Fig. 15). The phase transition from an inverse bicontinuous cubic to an inverted hexagonal

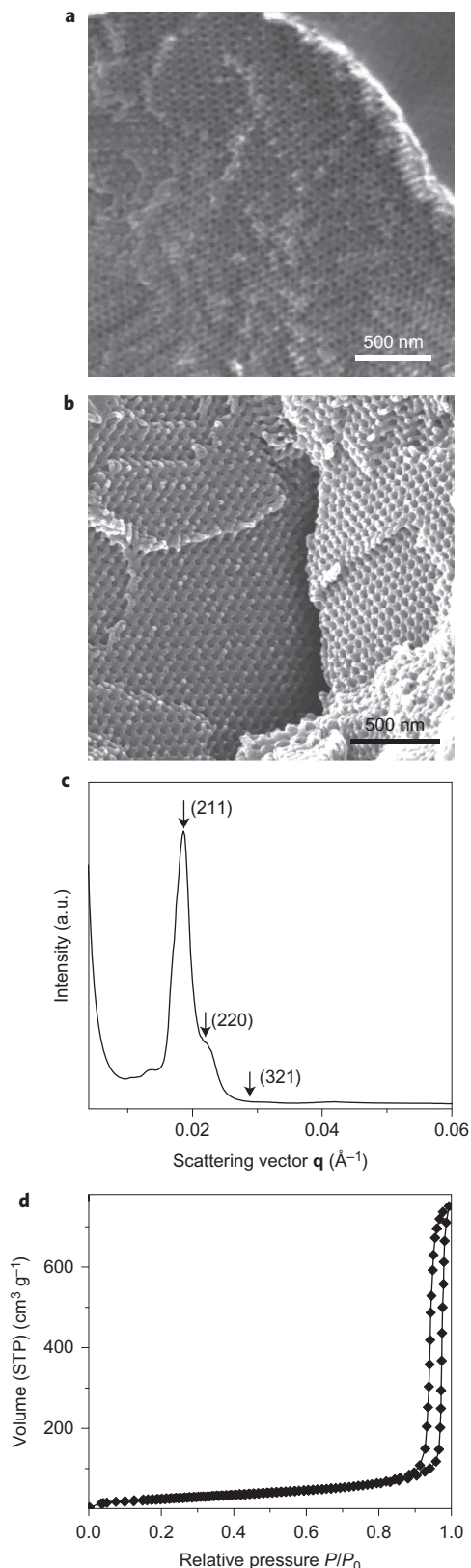


Figure 4 | Polymer cubosomes of **3₂₂₃.** **a,b,** HR-SEM images showing the internal double-gyroid structures of the polymer cubosome of **3₂₂₃** viewed in the [111] (**a**) and [110] (**b**) directions. **c,** SAXS results of dried polymer cubosomes of **3₂₂₃**. Peaks were assigned to *Ia3d* symmetry ($a = 82.3 \text{ nm}$). **d,** N_2 adsorption-desorption isotherms of the dried polymer cubosomes of **3₂₂₃** measured at 77 K (BET surface area $99 \text{ m}^2 \text{ g}^{-1}$, pore volume $1.16 \text{ cm}^3 \text{ g}^{-1}$).

phase was more pronounced when, for example, **1₂₃₂** was self-assembled in the presence of homo-PS ($M_n = 12,000 \text{ g mol}^{-1}$) as an additive (10% w/w). As shown from lipidic assemblies³⁹, an increase in the volume fraction of the hydrophobic compartment, caused by added hydrophobes, induced a complete phase transition of the internal structure into an inverted hexagonal internal phase, which was observed by SEM and TEM (Supplementary Fig. 16). These results indicated that self-assembled structures of dendritic-linear block copolymers undergo a morphological transition from bilayer lamellae and vesicles to inverse bicontinuous cubic structures and inverse hexagonal structures on a gradual decrease of f_{PEG} values.

Surface functionalization of polymer cubosomes. The polymer cubosomes reported here had a well-defined internal structure that consisted of interconnected networks of water channels arranged in a cubic crystalline order and with a surface area in excess of $100 \text{ m}^2 \text{ g}^{-1}$. The perforated outer shell connected the internal networks of large water channels to the surroundings in all directions. To utilize the internal volume of the polymer cubosomes to accommodate large guests, such as enzymes and protein complexes, we introduced functional groups on the surface of the bilayer membranes that constituted the polymer cubosomes via the coassembly of **1₂₁₇** and linear block copolymers that possess an α -amino (NH_2)- or thiol (SH)-functionalized PEG block ($\text{NH}_2\text{-PEG}_{45}\text{-PS}_{210}$, SH-PEG₄₅-PS₂₁₀, $M_n = 23,000 \text{ g mol}^{-1}$, $f_{\text{PEG}} = 9.2\%$) (Supplementary Fig. 6)⁴¹. The coassembly of **1₂₁₇** with these end-functionalized block copolymers (up to 10% w/w) did not disrupt the crystalline lattices of the resulting functionalized polymer cubosomes as observed by SEM and TEM (Fig. 5 and Supplementary Fig. 18). From the molecular areas of PEG₄₅-PS₂₁₀ (950 \AA^2) and **1₂₁₇** ($1,370 \text{ \AA}^2$) determined by Langmuir isotherms at the air–water interface, these polymer cubosomes could have up to $1.6 \mu\text{mol g}^{-1}$ of surface functional groups if 10 wt% of the end-functionalized linear block copolymers were used for coassembly.

The successful incorporation of the functional groups on the internal surface of the polymer cubosomes was confirmed by confocal laser scanning microscopy (CLSM) after the covalent labelling of surface functional groups in phosphate buffer (pH 7.4) using fluorescein-5-maleimide (F-MI) for the SH groups and rhodamine-*N*-hydroxysuccinimidyl ester (Rho-NHS) for NH₂ groups (Fig. 5e). Also, these functional groups could be introduced into polymer cubosomes of **1₂₁₇** in tandem by using a mixture of NH₂-PEG₄₅-PS₂₁₀ and SH-PEG₄₅-PS₂₁₀ for coassembly. After orthogonally labelling these functional groups with an equimolar mixture of F-MI and Rho-NHS in buffer, the resulting polymer cubosomes showed fluorescence of both dyes on the CLSM, which confirmed the coexistence of both functional groups in the polymer cubosomes (Fig. 6a).

Once the presence of functional groups on the bicontinuous internal structure of the polymer cubosomes was established, we compartmentalized a protein guest, fluorescein-labelled streptavidin homotetramer, within the water channels of the polymer cubosomes of **1₂₁₇**/NH₂-PEG₄₅-PS₂₁₀ (10% w/w). The polymer cubosomes were first reacted with NHS-PEG₄-biotin to afford the surface-bound biotin acting as anchoring points of streptavidin via a strong non-covalent interaction between them. Fluorescein-labelled streptavidin homotetramer was internalized through the surface pores (average diameter $>10 \text{ nm}$ (Fig. 5b)) by mixing the protein solution with a suspension of the biotin-labelled polymer cubosomes (Fig. 6b). After purification, no retention of streptavidin was observed within the polymer cubosomes of **1₂₁₇**/NH₂-PEG₄₅-PS₂₁₀ without surface-bound biotin.

We also demonstrated that the polymer cubosomes could be a platform for biochemical reactors by internalizing the enzyme maleimide-activated horseradish peroxidase (HRP, 44.1 kDa) in the SH-functionalized polymer cubosomes (SH-PEG₄₅-PS₂₁₀/**1₂₁₇**,

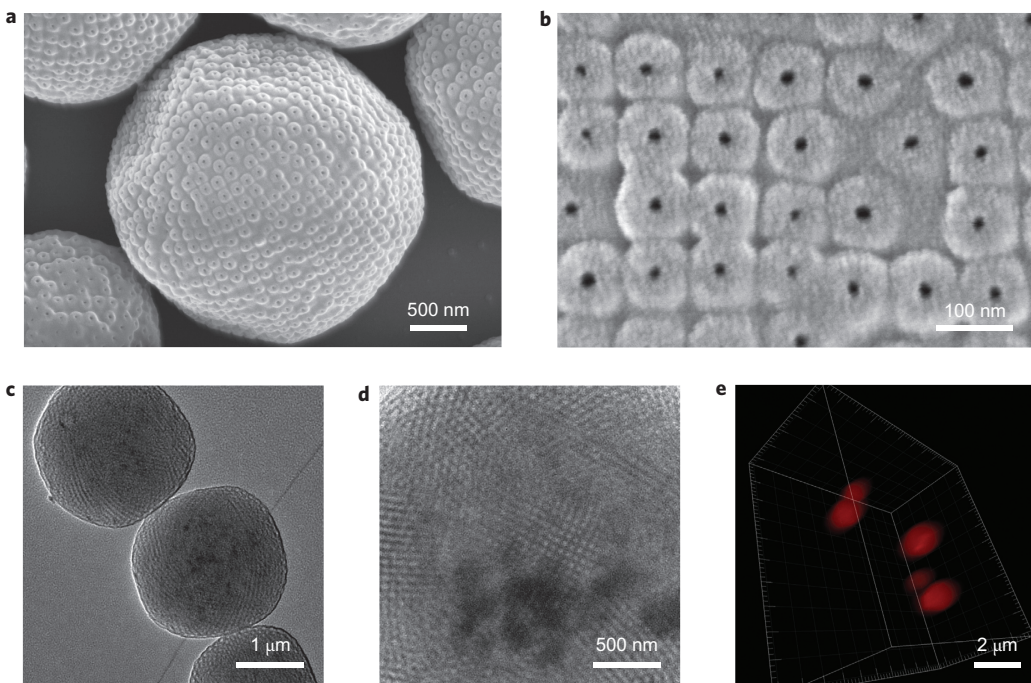


Figure 5 | Surface-functionalized polymer cubosomes. **a**, SEM image of polymer cubosomes obtained from the coassembly of **1₂₁₇** and NH₂-PEG₄₅-PS₂₁₀ (10% w/w). **b**, HR-SEM image showing the surface pores of the polymer cubosome of **1₂₁₇**/NH₂-PEG₄₅-PS₂₁₀ (10% w/w). **c,d**, TEM images showing the internal structures of the polymer cubosomes of **1₂₁₇**/NH₂-PEG₄₅-PS₂₁₀ (10% w/w). **e**, 3D reconstructed images of CLSM of the polymer cubosomes of **1₂₁₇**/NH₂-PEG₄₅-PS₂₁₀ (10% w/w) after the reaction with Rho-NHS.

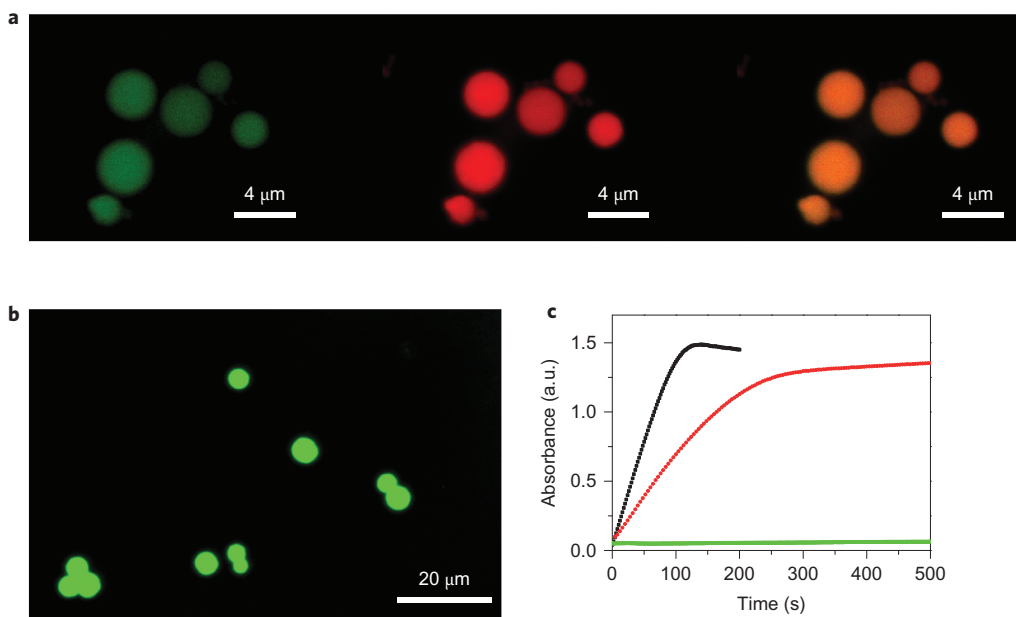


Figure 6 | Surface-functionalized polymer cubosomes. **a**, CLSM images of polymer cubosomes of **1₂₁₇** and NH₂-PEG₄₅-PS₂₁₀/SH-PEG₄₅-PS₂₁₀ (equimolar mixture, 8% w/w) after selectively labelling SH groups with F-MI ($\lambda_{\text{ex}} = 492$ nm, $\lambda_{\text{em}} = 518$ nm, left (ex, excitation; em, emission)) and NH₂ groups with Rho-NHS ($\lambda_{\text{ex}} = 564$ nm, $\lambda_{\text{em}} = 589$ nm, centre). The merged image confirmed the presence of both functional groups in the same polymer cubosome (right). **b**, CLSM image of fluorescein-labelled streptavidin within the biotin-labelled polymer cubosomes of **1₂₁₇**/NH₂-PEG₄₅-PS₂₁₀ (10% w/w). **c**, Time-course plots of the absorption of radical cation of ABTS^{•+} oxidized by free (black line) and HRP-cubosomes (red line) of SH-PEG₄₅-PS₂₁₀/**1₂₁₇** (7% w/w). Free HRP or HRP-cubosome was mixed with a solution containing 1.6 mM ABTS and 0.125 mM H₂O₂ in phosphate buffer (pH 7.4). The absorbance was measured at 740 nm. The green trace indicates the background absorption of ABTS and H₂O₂ in the absence of HRP.

7% w/w). The amount of surface-bound HRPs on the polymer cubosomes was quantified by inductively coupled plasma mass spectrometry (ICP-MS), which showed a value of 0.76 $\mu\text{mol g}^{-1}$ and indicated that about 70% of the surface SH groups were

functionalized. The presence of surface-bound HRP was confirmed by colorimetric assay conducted by the enzymatic oxidation of ABTS (2,2'-azinobis(3-ethylbenzothiazoline-6-sulfonic acid) diammonium salt) in the presence of H₂O₂ as an oxidant. From

the kinetic analysis of the oxidation of ABTS, the apparent Michaelis constant ($K_M = 0.29 \text{ mM}$) and maximum reaction rate ($V_{\max} = 0.005 \mu\text{M s}^{-1}$) were determined, which were reduced values in comparison to the measured values of free HRP solution at the same concentration (Fig. 6c and Supplementary Table 2). However, these catalytic constants were substantially higher than those reported in the literature for HRP physically adsorbed within the internal pores (7.6 nm diameter) of mesoporous silica particles (SBA-15)⁴². The fast kinetics of HRP bound at the end of the long PEG chain protruding from the internal surface of the polymer cubosomes suggests a low diffusion barrier in the polymer cubosomes promoted by the cubic networks of large water channels open to the environment.

In summary, we have shown that amphiphilic block copolymers built from a hydrophilic dendritic block directly self-assembled into colloidal particles of inverse bicontinuous membranes (polymer cubosomes) in aqueous solution. These polymer cubosomes exhibited highly defined crystalline internal structures of inverse bicontinuous cubic phases. Depending on the architecture of the dendritic scaffold in the hydrophilic block, we observed three bicontinuous cubic structures (double-diamond, gyroid and primitive cubic phases) analogous to the inverse bicontinuous phases observed from lipid assemblies. These polymer cubosomes were found to be mesoporous, as characterized by N₂-adsorption experiments. By coassembly with α -NH₂- or SH-functionalized linear block copolymers, our block copolymers formed highly defined mesoporous colloidal polymer structures with surface functional groups that can anchor external guests, such as proteins and enzymes.

These results demonstrate that the polymer cubosomes, mesoporous polymeric materials with unprecedented internal structural orders and tunable surface functionalities, may offer new platforms for bioreactors, storage vehicles, sensors and nanotemplates. Polymer cubosomes, which are directly formed from the simple solution self-assembly of block copolymers into inverse cubic mesophases, can be distinguished from most inorganic and polymeric porous materials, which are synthesized using sacrificial templates as pore generators. The architectures of block copolymers based on the dendritic hydrophilic block play a crucial role in the preferential formation of inverse cubic mesophases in solution; this resembles the formation of complex bilayers exhibited by lipids. Our report may open new avenues to investigate and utilize the interesting properties of inverse mesophases of block copolymers, which have not been widely available from the conventional solution self-assembly of block copolymers.

Methods

Synthetic procedures and characterization of dendritic macroinitiators and block copolymers used in this work are described in Supplementary Information.

Self-assembly of dendritic-linear block copolymers into polymer cubosomes. In a typical procedure, **1₂₁₇** (20 mg) was dissolved in 1,4-dioxane (2 ml) in a 15 ml capped vial with a magnetic stirrer. The solution was stirred for three hours at room temperature. A syringe pump was calibrated to deliver water at a speed of 1 ml h⁻¹. The vial cap was replaced by a rubber septum. Water (2 ml, MilliQ, 18.1 MΩ) was added to the organic solution with vigorous stirring (850 revolutions per minute) by a syringe pump with a 5 ml syringe equipped with a steel needle. The resulting suspension solution was subjected to dialysis (molecular weight cutoff (MWCO) ~12–14 kDa (SpectraPor)) against water for 24 hours with frequent changes of water. The procedure could be scaled up to 100 mg with a proportionally increased amount of solvents and rate of water addition. For coassembly with α -functionalized linear block copolymers, the block copolymer mixture was prepared by mixing dioxane solutions of a linear-dendritic block copolymer (10 mg ml⁻¹) and the α -functionalized linear block copolymer (2 mg ml⁻¹) in an appropriate ratio (2 ml). This mixture was stirred for three hours at room temperature. Water was added to it via a syringe pump, as described above, followed by dialysis against water. Polymer cubosomes settled down in water during storage under gravity, and could be redispersed on shaking the aqueous solution.

Covalent labelling of surface functional groups of polymer cubosomes. An equimolar mixture of Rho-NHS and F-MI was dissolved in PBS (pH 7.4). This solution was mixed with the polymer cubosomes of **1₂₁₇**(NH₂-PEG₄₅-

PS₂₁₀/SH-PEG₄₅-PS₂₁₀) (an equimolar mixture of linear block copolymers, 8% w/w) dispersed in PBS. The mixture was aged for 16 hours at room temperature. The excess fluorescent dyes were removed from the suspension by repeated centrifugation on a centrifugal filter (MWCO = 100 kDa (Amicon)) and dilution with buffer and methanol until the aliquot did not show any fluorescence. The polymer cubosomes of **1₂₁₇** without surface functional groups did not show any retention of dyes on fluorescence microscopy after the same procedure of purification. The labelled polymer cubosomes were visualized on a confocal laser scanning microscope (FluoView 1000, Olympus).

Biotinylation of polymer cubosomes and streptavidin compartmentalization.

The polymer cubosomes of **1₂₁₇**(NH₂-PEG₄₅-PS₂₁₀) (10% w/w) were prepared by the method described above. The NH₂-functionalized polymer cubosomes were reacted with NHS-PEG₄-biotin (Thermo Scientific) in PBS (pH 7.4) for 24 hours at room temperature. The excess reagent was removed from the suspension by repeated centrifugation and dilution with PBS and methanol. These biotin-polymer cubosomes were mixed with a PBS solution of fluorescein-labelled streptavidin homotetramer (Sigma) for 24 hours at 4 °C. The unbound streptavidin was removed by centrifugation on a centrifugal filter (MWCO = 100 kDa (Amicon)). The centrifugation was repeated until the filtered portion showed no fluorescence.

Conjugation of HRP to polymer cubosomes. A PBS solution of the cubosome of **1₂₁₇**(SH-PEG₄₅-PS₂₁₀) (7% w/w, 1 mg ml⁻¹, pH 7.4) was added to HRP-maleimide (1 mg, 44.1 kDa) in a vial. The mixture was stirred for three days. The solution was then centrifuged and washed several times with PBS solution until no free HRP could be detected in the supernatant. As detected by ICP-MS, about 70% of all available thiol sites were occupied by HRP-maleimide. To measure the enzymatic activity, equivalent amounts of HRP from free HRP or HRP-cubosome were mixed with a PBS solution (pH 7.4) of 1.67 mM ABTS in a quartz cell, and 0.125 mM hydrogen peroxide was added to initiate the oxidative reaction. Time-course absorption changes of ABTS^{•+} at 740 nm were collected on a JASCO V-670 spectrophotometer. The Michaelis-Menten equation was applied and the kinetic parameters were interpreted using a Lineweaver-Burk plot.

Received 22 July 2013; accepted 4 April 2014;
published online 11 May 2014

References

1. Israelachvili, J. N. *Intermolecular and Surface Forces* (Academic Press, 1992).
2. Zhang, L. & Eisenberg, A. Multiple morphologies of "crew-cut" aggregates of polystyrene-*b*-poly(acrylic acid) block copolymers. *Science* **268**, 1728–1731 (1995).
3. Zhang, L., Bartels, C., Yu, Y., Shen, H. & Eisenberg, A. Mesosized crystal-like structure of hexagonally packed hollow loops by solution self-assembly of diblock copolymers. *Phys. Rev. Lett.* **79**, 5034–5037 (1997).
4. Yu, K., Bartels, C. & Eisenberg, A. Trapping of intermediate structures of the morphological transition of vesicles to inverted hexagonally packed rods in dilute solutions of PS-*b*-PEO. *Langmuir* **15**, 7157–7167 (1999).
5. Mai, Y. & Eisenberg, A. Self-assembly of block copolymers. *Chem. Soc. Rev.* **41**, 5969–5985 (2012).
6. Schacher, F. H., Rupar, P. A. & Manners, I. Functional block copolymers: nanostructured materials with emerging applications. *Angew. Chem. Int. Ed.* **51**, 7898–7921 (2012).
7. Moffit, M., Khougaz, K. & Eisenberg, A. Micellization of ionic block copolymers. *Acc. Chem. Res.* **29**, 95–102 (1996).
8. Hales, K., Chen, Z., Wooley, K. L. & Pochan, D. J. Nanoparticles with tunable internal structure from triblock copolymers of PAA-*b*-PMA-*b*-PS. *Nano Lett.* **8**, 2023–2026 (2008).
9. Cui, H., Chen, Z., Zhong, S., Wooley, K. L. & Pochan, D. J. Block copolymer assembly via kinetic control. *Science* **317**, 647–650 (2007).
10. Li, Z., Kesselman, E., Talmon, Y., Hillmyer, M. A. & Lodge, T. P. Multicompartment micelles from ABC Miktoarm stars in water. *Science* **306**, 98–101 (2004).
11. Christian, D. A. *et al.* Spotted vesicles, striped micelles and Janus assemblies induced by ligand binding. *Nature Mater.* **8**, 843–849 (2009).
12. Wang, X. *et al.* Cylindrical block copolymer micelles and co-micelles of controlled length and architecture. *Science* **317**, 644–647 (2007).
13. Jackson, E. A. & Hillmyer, M. A. Nanoporous membranes derived from block copolymers: from drug delivery to water filtration. *ACS Nano* **4**, 3548–3553 (2010).
14. Seo, M. & Hillmyer, M. A. Reticulated nanoporous polymers by controlled polymerization-induced microphase separation. *Science* **336**, 1422–1425 (2012).
15. Peinemann, K-V., Abetz, V. & Simon, P. F. W. Asymmetric superstructure formed in a block copolymer via phase separation. *Nature Mater.* **6**, 992–996 (2007).
16. Larsson, K. Cubic lipid–water phases: structures and biomembrane aspects. *J. Phys. Chem.* **93**, 7304–7314 (1989).
17. Kulkarni, C. V., Wachter, W., Iglesias-Salto, G., Engelskirchen, S. & Ahualli, S. Monolein: a magic lipid? *Phys. Chem. Chem. Phys.* **13**, 3004–3021 (2011).

18. Almsherqi, Z. A., Kohlwein, S. D. & Deng, Y. Cubic membranes: a legend beyond the Flatland of cell membrane organization. *J. Cell Biol.* **173**, 839–844 (2006).
19. Lindström, M., Ljusberg-Wahren, H. & Larsson, K. Aqueous lipid phases of relevance to intestinal fat digestion and absorption. *Lipids* **16**, 749–754 (1981).
20. van Meer, G., Voelker, D. R. & Freigenson, G. W. Membrane lipids: where they are and how they behave. *Nature Rev. Mol. Cell Biol.* **9**, 112–124 (2008).
21. Gustafsson, J., Ljusberg-Wahren, H., Almgren, M. & Larsson, K. Cubic lipid–water phase dispersed into submicron particles. *Langmuir* **12**, 4611–4613 (1996).
22. Spicer, P. T. in *Dekker Encyclopedia of Nanoscience and Nanotechnology* (eds Schwarz, J. A., Contescu, C. & Putyera, K.) 881–892 (Marcel Dekker, 2004).
23. Landau, E. M. & Rosenbusch, J. P. Lipidic cubic phases: a novel concept for the crystallization of membrane proteins. *Proc. Natl Acad. Sci. USA* **93**, 14532–14535 (1996).
24. Caffrey, M. Crystallizing membrane proteins for structure determination: use of lipidic mesophases. *Ann. Rev. Biophys.* **38**, 29–51 (2009).
25. Angelova, A., Angelov, B., Papahadjopoulos-Sternberg, B., Ollivon, M. & Bourgaux, C. Proteocubosomes: nanoporous vehicles with tertiary organized fluid interfaces. *Langmuir* **21**, 4138–4143 (2005).
26. Spicer, P. T. Progress in liquid crystalline dispersions: cubosomes. *Curr. Opin. Colloid Interfac. Sci.* **10**, 274–279 (2005).
27. Battaglia, G. & Ryan, A. J. Effect of amphiphile size on the transformation from a lyotropic gel to a vesicular dispersion. *Macromolecules* **39**, 798–805 (2006).
28. Battaglia, G. & Ryan, A. J. The evolution of vesicles from bulk lamellar gels. *Nature Mater.* **4**, 869–876 (2005).
29. Jain, S., Gong, X., Scriven, L. E. & Bates, F. S. Disordered network state in hydrated block-copolymer surfactants. *Phys. Rev. Lett.* **96**, 138304 (2006).
30. Alexandridis, P., Olsson, U. & Lindman, B. Structural polymorphism of amphiphilic copolymers: six lyotropic liquid crystalline and two solution phases in a poly(oxybutylene)-*b*-poly(oxyethylene)-water-xylene system. *Langmuir* **13**, 23–34 (1997).
31. Percec, V. et al. Self-assembly of Janus dendrimers into uniform dendrimersomes and other complex architectures. *Science* **328**, 1009–1014 (2010).
32. McKenzie, B. E., Nudelman, F., Bomans, P. H. H., Holder, S. J. & Sommerdijk, N. A. J. M. Temperature-responsive nanospheres with bicontinuous internal structures from a semicrystalline amphiphilic block copolymer. *J. Am. Chem. Soc.* **132**, 10256–10259 (2010).
33. Parry, A. L., Bomans, P. H. H., Holder, S. J., Sommerdijk, N. A. J. M. & Biagini, S. C. G. Cryo electron tomography reveals confined complex morphologies of tripeptide-containing amphiphilic double-comb diblock copolymers. *Angew. Chem. Int. Ed.* **47**, 8859–8862 (2008).
34. Dehsorkhi, A., Castelletto, V., Hamley, I. W. & Harris, P. J. F. Multiple hydrogen bonds induce formation of nanoparticles with internal microemulsion structure by an amphiphilic copolymer. *Soft Matter* **7**, 10116–10121 (2011).
35. Denkova, A. G., Bomans, P. H. H., Coppens, M.-O., Sommerdijk, N. A. J. M. & Mendes, E. Complex morphologies of self-assembled block copolymer micelles in binary solvent mixtures: the role of solvent–solvent correlations. *Soft Matter* **7**, 6622–6628 (2011).
36. McKenzie, B. E., Holder, S. J. & Sommerdijk, N. A. J. M. Assessing internal structure of polymer assemblies from 2D to 3D cryoTEM: bicontinuous micelles. *Curr. Opin. Colloid Interface Sci.* **17**, 343–349 (2012).
37. Jeong, M. G., van Hest, J. C. M. & Kim, K. T. Self-assembly of dendritic–linear block copolymers with fixed molecular weight and block ratio. *Chem. Commun.* **48**, 3590–3592 (2012).
38. Kim, K. T. et al. Polymersome stomatocytes: controlled shape transformation of polymer vesicles. *J. Am. Chem. Soc.* **132**, 12522–12524 (2010).
39. Almgren, M., Edwards, K. & Karlsson, G. Cryo transmission electron microscopy of liposomes and related structures. *Colloid Surf. A* **174**, 3–21 (2000).
40. Kulkarni, C. V. et al. Engineering bicontinuous cubic structures at the nanoscale—the role of chain splay. *Soft Matter* **6**, 3191–3194 (2010).
41. Georgieva, J. V. et al. Peptide-mediated blood–brain barrier transport of polymersomes. *Angew. Chem. Int. Ed.* **51**, 8339–8342 (2012).
42. Ikemoto, H., Chi, Q. & Ulstrup, J. Stability and catalytic kinetics of horseradish peroxidase confined in nanoporous SBA-15. *J. Phys. Chem. C* **114**, 16174–16180 (2010).

Acknowledgements

This research was supported by the National Research Foundation (NRF) of Korea (NRF-2013R1A1A013075) and Ulsan National Institute of Science and Technology (2012 Future Challenge Research Fund, 1.130014). C.P. acknowledges the NRF for a research fellowship (2013R1A1A2063049). S.H.J. and S.K. thank NRF for financial support (2013R1A1A2012960, ARC 2010-0028684). K.T.K also thanks KUCC for financial support (2V03280). We thank the Unist Central Research Facilities and the Unist-Olympus Biomed Imaging Center for microscopy facilities. We thank J. Y. Cheon and Y. J. Kang for the help with adsorption experiments and protein labelling. We also thank M. G. Jeong for the graphical illustrations.

Author contributions

K.T.K. conceived and designed the experiments. Y.L. carried out most of the experiments, C.P. performed the experiments on surface functionalization and T.J.S. conducted SAXS experiments. S.H. Joo and S.K. carried out porosimetry and protein labelling. All the authors contributed to the analysis and interpretation of the data. K.T.K. wrote the manuscript. All the authors commented on the manuscript.

Additional information

Supplementary information is available in the online version of the paper. Reprints and permissions information is available online at www.nature.com/reprints. Correspondence and requests for materials should be addressed to K.T.K.

Competing financial interests

The authors declare no competing financial interests.